

Modes of Oscillation in a Nonreacting Ramjet Combustor Flow

Wen-Huei Jou* and Suresh Menon†
Quest Integrated, Inc., Kent, Washington 98032

The results of the numerical simulation of cold flows in a ramjet are used to identify the mechanism that leads to the observed pressure fluctuations. The acoustic disturbance is defined as the unsteady part of the potential field and is shown to be driven by the instantaneous dilatation field. The quadrupole nature of the sound source around each vortex in the flowfield is demonstrated. The dilatation field in the vortex impingement region on the nozzle wall is considered a compact acoustic source and is analyzed by multipole expansion of the distributed field, revealing a strong axial acoustic dipole 180 deg out of phase with the impinging vorticity fluctuations. This dipole response to the vortical fluctuation is applied as the impedance for the vorticity/acoustic fluctuations at the nozzle. The spectral analysis of pressure and vorticity fluctuations reveals both a resonant acoustic mode in which the vortical disturbances excite the acoustic free modes, and a coupled mode in which the acoustic and vortical disturbances are coupled through dipole radiation at the nozzle and the acoustic susceptibility of the separating shear layer at the dump plane. A model for the coupled mode is proposed that provides a method for estimating its frequency.

Introduction

RAMJETS are known to be unstable under certain operating conditions. Many studies show that vortex shedding at the flameholder is a major factor in this instability. In a recent study,¹ a numerical method for simulation of the unsteady flow in an axisymmetric ramjet combustor has been developed. In particular, the proper boundary conditions and the accuracy of the computations were addressed. Simulations of cold flows in a ramjet combustor with a choked exhaust nozzle were performed. It was found that the axisymmetric shear layer is unstable, and that concentrated vortices are formed by the rollup of the vortex sheet. The subsequent merging of these vortices contributes to the growth of the thickness of the mixing layer. The contribution of these large coherent structures to the global transport of momentum was computed by the evaluation of various mean flow quantities from the simulation data. For unsteady aspects of the flow, the pressure-time history at various locations in the combustor indicated that coherent pressure fluctuations exist in the combustor, although the amplitudes are small.

The present paper concentrates on the analysis of the simulation results and on extracting detailed information on the physical processes leading to the coherent pressure fluctuation in the dump combustor. The methodology used to extract acoustic information from the results of numerical simulations is described. In particular, the nature of the acoustic source resulting from the vortex/choked-nozzle interaction is uncovered. Based on the information extracted from the simulations, possible mechanisms for pressure oscillations in a dump combustor are described. In particular, the differentiation between resonant oscillations and coupled-mode oscillations is made. Although the former has been widely recognized by researchers, the detailed mechanism of the latter is

less understood and requires further investigation. In this paper, a model is constructed to explain the coupled-mode oscillations and to make some preliminary estimates of the characteristic frequency of the coupled modes.

Extracting Acoustic Information

The major difference between the present simulations and the direct numerical simulations of incompressible turbulent flows extensively investigated in the past^{2,3} is the existence of acoustic disturbances in the computational domain when the reduced frequency of the system based on the speed of sound is of the order of unity.¹ New methods must be developed to extract acoustic information from the results of numerical simulations in order to uncover physical phenomena associated with the compressibility effects.

In a linearized analysis by Chu and Kovasznay,⁴ it was shown that the propagation of small disturbances in a compressible fluid can be decomposed into three canonical components. One of these components consists of the acoustic waves, with the speed of sound as the characteristic velocity. The other two are the entropy wave and the vorticity wave. Their characteristic velocity is the fluid velocity, and thus they are called convective waves. This theory is applied to disturbances in an infinite space. It can also be applied to localized disturbances where the boundary conditions are not considered.

For flows in a finite space, as in a ramjet combustor, boundary conditions are an important element of the problem. The decomposition of the linear disturbance into canonical components must consider the appropriate boundary conditions that may result in coupling among the free wave components. Furthermore, large-amplitude nonlinear disturbances, such as vorticity fluctuations resulting from the instability of a shear layer, may occur in a ramjet combustor. This is evident from the numerical simulations, as demonstrated in the accompanying article.¹ The notion of an acoustic wave defined by a linearized analysis, such as that of Chu and Kovasznay,⁴ serves as a conceptual guideline for developing methods of interpreting physical processes in a nonlinear system. In a nonlinear near field, however, the definition of an acoustic disturbance requires clarification. A clear definition of an acoustic disturbance applicable to a nonlinear system is necessary for the consistent analysis and interpretation of the results of numerical simulations.

Presented as Paper 87-1422 at the AIAA 19th Fluid Dynamics, Plasma Dynamics, and Lasers Conference, Honolulu, HI, June 8-10, 1987; received Nov. 28, 1988; revision received Sept. 11, 1989. Copyright © 1990 by the American Institute of Aeronautics and Astronautics, Inc. All rights reserved.

*Vice President, Applied Mechanics Division; currently, Manager, CFD Development, Boeing Commercial Airplane Group, Seattle, WA.

†Senior Research Scientist. (Quest Integrated, Inc., was formerly Flow Research, Inc.)

Since an acoustic disturbance is identified with the unsteady potential flow in a linearized system, it is natural to attempt to define the acoustic disturbance in terms of the velocity field. It is well known (e.g., Goldstein⁵) that a vector field \mathbf{u} can be decomposed into a solenoidal field \mathbf{v} and a potential component $\nabla\phi$ as

$$\mathbf{u} = \mathbf{v} + \nabla\phi \quad (1)$$

The solenoidal field \mathbf{v} satisfies the incompressible condition

$$\nabla \cdot \mathbf{v} = 0 \quad (2)$$

and the vorticity of the velocity field \mathbf{u} is included by \mathbf{v} to satisfy the following relation:

$$\nabla \times \mathbf{v} = \nabla \times \mathbf{u} = \Omega \quad (3)$$

A similar approach was taken by Flandro⁶ to separate the vortical motion and the irrotational acoustic oscillations. From Eq. 3 the vorticity Ω can be identified as the source term in determining the vortical component of the velocity field \mathbf{v} . In particular, a stream function ψ can be defined for the solenoidal field \mathbf{v} in two-dimensional or axisymmetric flows so that

$$\nabla^2\psi = -\Omega \quad (4)$$

where the vorticity is the source term for determining the vortical stream function ψ .

Although the solenoidal field contains all of the vortical field of the given velocity field, the potential field ϕ includes all of the dilatation field of \mathbf{u} . Therefore,

$$\nabla^2\phi = \nabla \cdot \mathbf{u} = \Delta \quad (5)$$

where Δ is the dilatation field. This decomposition is arbitrary up to a solenoidal-potential field. In other words, the classification of an irrotational-incompressible flowfield into one of the two components is arbitrary. This decomposition of the velocity field is kinematic in nature and is valid for both the linear and nonlinear cases.

The definition of acoustic disturbance is given as the unsteady portion of the velocity potential.^{7,8} Goldstein⁵ further constrained this decomposition by defining the vortical velocity as that governed by a pure convective equation. The pressure variation is attributed to the "acoustic" velocity field. This constraint attaches dynamic significance to the original kinematic decomposition, and therefore the arbitrariness in the decomposition of the velocity field in Eq. (1) is removed.

Subtracting the time-averaged part from Eq. (5), the equation for the acoustic potential ϕ' can be given as

$$\nabla^2\phi' = \Delta - \langle \Delta \rangle = \Delta' \quad (6)$$

where the instantaneous fluctuating dilatation field Δ' acts as a source.

In analyzing the results of the numerical simulations described earlier,¹ the vorticity contour field was used as a representative quantity for visualization of the vortical disturbance in the flowfield. From the parallel between Eqs. (4) and (6), it appears that the unsteady part of the dilatation field may serve as a representative quantity for visualizing the acoustic disturbance.

In the numerical simulations, the dilatation field is computed at each time step. A time average of the dilatation field for the simulation time period is performed. The mean field is then subtracted from the instantaneous field to obtain the instantaneous fluctuating component. Typical contours of the instantaneous dilatation field in the combustor are shown in Fig. 1. Two regions of high instantaneous dilatation field are identified and analyzed in detail below.

The first region is the shear layer near the dump plane where the rollup occurs. A careful examination of the dilatation and vorticity fields in this region reveals that the dilatation field around each concentrated vortex is a quadrupole. Figures 2a and 2b show closeups of the vorticity field and the corresponding dilatation field, respectively, near the dump plane. The quadrupole nature of the dilatation field around a rollup vortex is clearly shown. This visual pattern of the dilatation field travels with the vorticity pattern, which contradicts the general notion of an acoustic disturbance.

Consider Lighthill's acoustic analogy⁹:

$$\frac{1}{c^2} \frac{D^2\phi}{Dt^2} - \nabla^2\phi = S \quad (7)$$

The source term S of this equation involves the fluctuation of the "Bernoulli enthalpy."^{10,11} For the present case, in which combustion is absent, this source term consists mainly of the vortical disturbances. In the near field, these sources are not negligible. The length and time scales of the sources dominate this region so that the acoustic Eq. (7) must be scaled accordingly. It follows immediately that the first term of the acoustic equation is of $\mathcal{O}(M^2)$ as compared to the other terms and is negligible in low subsonic flows. The acoustic potential is governed by a Poisson's equation with vorticity disturbances acting as a source term. The propagation aspects of the acoustic wave are lost under this scaling, and the acoustic potential field, which is dominated by the sources in the near field, travels at the characteristic velocity of a vortical field rather than at the speed of sound. This is usually called a pseudo-sound¹² and is not an acoustic wave in the conventional sense. The quadrupole behavior of the dilatation field around a concentrated vortex essentially reflects the source behavior discussed by Lighthill.⁹ It is worthwhile to mention that the quadrupole sources are weak radiators of sound, and perhaps the resulting acoustic waves interact only weakly with the vortical motion. The same conclusion was arrived at by Flandro.⁶

The visualization of the dilatation field probably can be used to detect a propagating short acoustic wave such as a shock wave. In general, the long wave in a subsonic flow is difficult to visualize by this method. If the short-wavelength

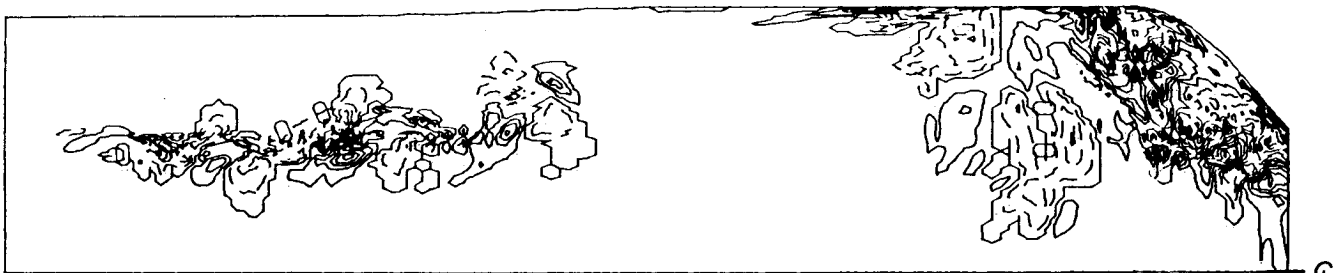


Fig. 1 The instantaneous dilatation field in the combustor for $M = 0.32$ and $Re_D = 1 \times 10^4$. The computational grid resolution is 256×64 , and the contour interval is 200 s^{-1} .

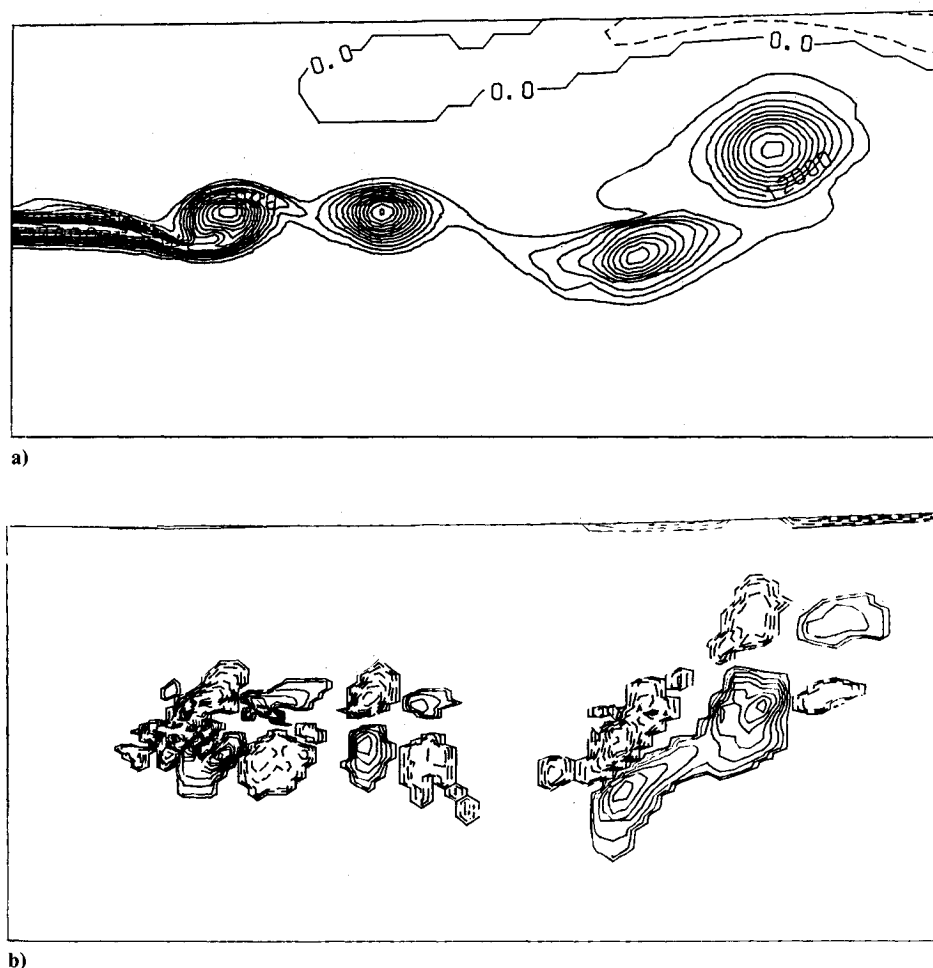


Fig. 2 Comparison of vorticity and dilatation field near the dump plane. Conditions same as in Fig. 1: a) vorticity contours at interval of 3000 s^{-1} ; and b) dilatation contours at interval of 150 s^{-1} .

pseudosound disturbances caused by the vortical field can be filtered from the computed dilatation field, the long acoustic wave may be revealed. This filtering process requires integration of the dilatation field over a sampling volume that is small compared to the wavelength and yet large compared to the scale of the vortical disturbance. In the simulations, a suitable spatial average over a sampling volume is difficult to define, and the deduction of long acoustic waves from the results of simulations has not been attempted.

The dilemma of separating acoustic information from the vortical disturbances, as demonstrated by the pseudosound discussed above, is not new. Crow¹¹ posed the problem of the formulation of an acoustic equation as follows: given a vorticity field Ω , find the density field and the velocity potential. He considered the subsonic cases in which the eddy length scale and the length scale of the region of vortical disturbances are much smaller than the acoustic wavelength. The acoustic analogy of Lighthill⁹ is the result of a matched asymptotic expansion based on the smallness of the characteristic lengths in comparison to the acoustic wavelength. For a source region with dimensions comparable to the wavelength, he concluded that the separation of the acoustic disturbance from the vortical disturbance is dubious. Although it is purely speculative, a multiple-scale expansion may lead to a better formulation for the problem in which the region of vortical disturbances is as large as the acoustic wavelength, whereas the eddy size remains small. This is, of course, beyond the scope of the present work.

Since the dilatation in the near field is dominated by the pseudosound and since the propagation aspects of acoustic waves are difficult to isolate for a low subsonic flow, the

dilatation field is used to define the characteristics of the acoustic sources only in the near field. The detection of a long-wavelength acoustic disturbance in the numerical simulations relies mainly on the temporal record of pressure fluctuations at locations where the vortical disturbances are believed to be small.

The second region of high instantaneous dilatation field is near the location where the coherent vortical structures impinge on the solid surface. The structure of the dilatation field in that region is also very complex. Figure 3 provides a comparison between the vorticity and dilatation fields near the nozzle region for two points in time during the simulation. If the eddy size is small compared to the acoustic wavelength, the source can be considered compact. Its behavior can be represented by a multipole expansion of the distributed sources.⁵ The lower-order singular sources are known to be more effective sound radiators than quadrupoles. The strengths of the first two terms of the expansion can be determined by taking spatial moments of the distributed dilatation field over a sampling volume. The strength of the monopole q_0 and the dipole q_1 can be computed by the following integrals:

$$q_0 = \int_V \Delta' \, dx \quad (8)$$

$$q_1 = - \int_V \Delta' x \, dx + \frac{q_0}{V} \int_V x \, dx \quad (9)$$

where V is the sampling volume containing the vortex impingement region. The time variation of the strength of the monopole and the axial component of the dipole together with

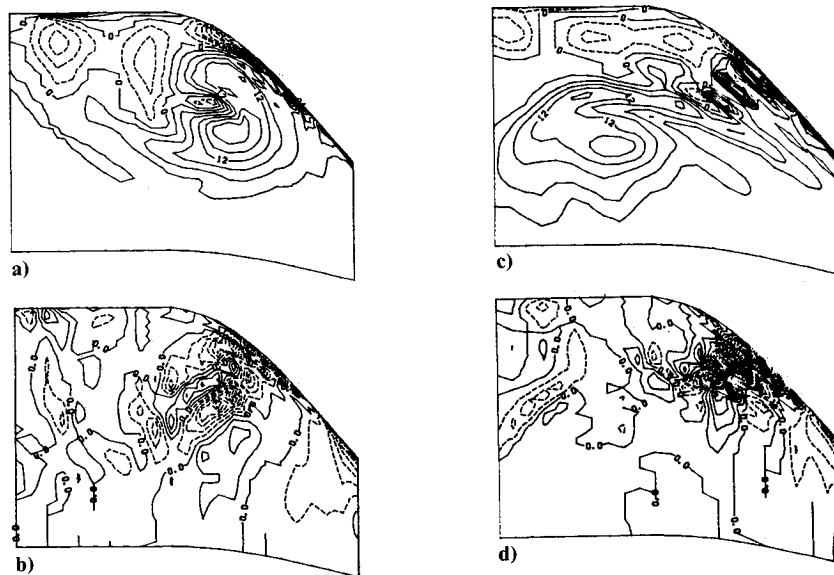


Fig. 3 Comparison of vorticity and dilatation fields in the nozzle. Conditions same as in Fig. 1: a) vorticity field; b) dilatation field; c) vorticity field; and d) dilatation field.

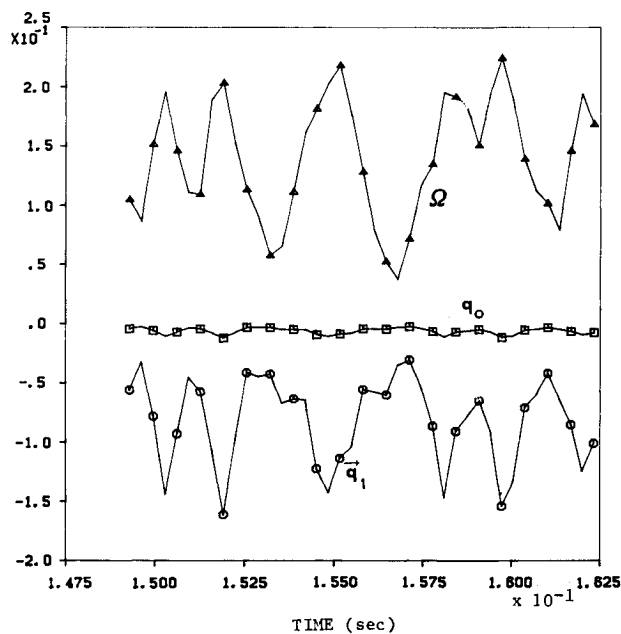


Fig. 4 Time variation of the nondimensional vorticity Ω , acoustic monopole q_0 , and acoustic dipole q_1 in the nozzle region.

the vorticity integrated over the same volume are displayed in Fig. 4 to show their relationship. It appears that, as the large vortical structure impinges on the wall, a strong fluctuating dipole is generated there. The dipole field is 180 deg out of phase with the vorticity fluctuation.

In carefully performed wind-tunnel experiments, Wills¹³ observed upstream propagating acoustic disturbances generated at the downstream diffuser even at a low flow speed of 38 m/s. Crighton,⁷ in studying the problem of "excess jet noise," found that turbulence causes a fluctuation in the thrust of a jet that is acoustically equivalent to a strong dipole, and that the unsteady mass flux corresponds to a weak monopole. Flandro⁶ postulated that the drag on a constriction in a combustion chamber is equivalent to the body force in the flowfield. By incorporating this body force into the momentum equation, the effect of the constriction on acoustic disturbance can be shown to be a dipole. In the present problem, the interaction between the impinging vortices and the nozzle causes fluctuat-

ing forces on the nozzle. Acoustically, the fluctuating force is equivalent to a dipole, as shown by the preceding analysis. These results provide some insight into the nature of sound generation due to vortex impingement on a nozzle. This knowledge of the acoustic behavior of the nozzle resulting from the interaction between impinging vortices and the nozzle can be used to construct a model for the pressure oscillations, as will be discussed in the following two sections.

The major finding presented in this section is that the instantaneous dilatation field is the appropriate quantity to represent the acoustic field. It was also found, however, that the near-field dilatation is dominated by the pseudosound and therefore represents the source behavior. If the sources are assumed compact, Eqs. (8) and (9) can be used to find the acoustic monopole and dipole sources in the flowfield. Quadrupole sources are considered weak radiators and are neglected.

Mode of Oscillations

In the preceding section, the attempt to extract acoustic information from the results of simulations was discussed. The propagation aspect of the long acoustic wave, however, is difficult to isolate. Therefore, point pressure data may be a better representative quantity for the analysis of long acoustic waves. The power spectra of various flow quantities computed at a set of discrete points in the flowfield are analyzed to provide further information on the fluctuating field. The flow quantities chosen for analysis are the vorticity and the pressure. The first quantity represents the vortical component of the flowfield, whereas the second quantity is more ambiguous. Again, in the near field, both the vortical component and the acoustic component, if such a distinction can still be made, contribute simultaneously to the fluctuation of the static pressure. As Ffowcs Williams pointed out,¹⁴ the low-frequency components of the pressure fluctuation must contain acoustic waves. There are locations in the combustor where the vorticity is locally at a very low level. Because the flow is locally a potential flow, the pressure fluctuations computed there are assumed to represent acoustic oscillations. Since the acoustic wavelength is comparable to the length of the combustor, the Biot-Savart law may not give the correct phase relation between the source and the pressure fluctuation at the dump plane. The Biot-Savart law is applicable only when the acoustic wavelength for the given frequency is much larger than the distance between an observer and the source. In the present simulations, the pressure fluctuation at the base of the back-

ward-facing step, where the vorticity fluctuation is small, is considered an acoustic fluctuation.

Figure 5a shows the computed spectrum of pressure at the base of the step. The Mach number in the inlet duct for this simulation is 0.32. There are three distinct peaks in the spectrum at approximately 650, 370, and 180 Hz. Although the level of the pressure oscillations is low, at only 4% of the static pressure, the existence of peaks at these distinct frequencies deserves careful consideration.

There are several ways in which vortical motions of the fluid elements can contribute to the coherent acoustic oscillations. The easiest mechanism to identify is that of a resonant oscillation. Consider Lighthill's acoustic analogy,⁹ as shown in Eq. (7). The vortices are considered a source independent of acoustic waves. Their presence merely excites the acoustic disturbances. When the space-time distribution of the sources contains one of the "free modes" defined by the eigensolutions of the homogeneous acoustic equation and boundary conditions, a resonant condition is satisfied. The acoustic oscillations in the duct accumulate, and large-amplitude oscillations may result. The frequency of this class of oscillations is that of a free mode.

There is another mechanism by which vortical disturbances can cause pressure fluctuations in a bounded domain such as a dump combustor. In this mechanism, a vortical disturbance may couple with the acoustic disturbance at the boundary to form a type of oscillation in which the vortical disturbance is part of the eigenvector and in which the frequency depends on the eigenvalue of the combined vortical/acoustic wave operator and therefore also depends strongly on the phase speed of the vortical disturbance. This coupling between vorticity and acoustic waves at the solid boundary was discussed in its linearized form by Goldstein⁵ in his general discussion of the sound generated by a blade row. This type of oscillation is referred to as coupled-mode oscillation. The detailed mechanisms of this mode will be discussed in the next section using a simple model.

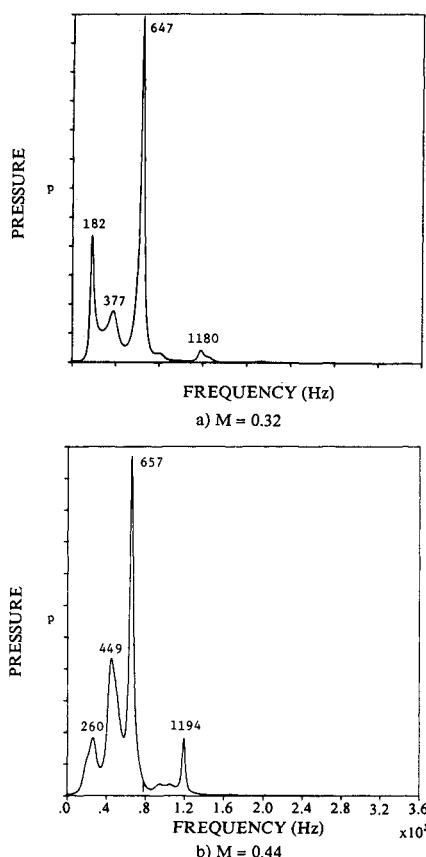


Fig. 5 Pressure spectra at the base of the step. The computational grid is 192×64 and $Re_D = 5 \times 10^3$: a) $M = 0.32$; and b) $M = 0.44$.

The following simulation method was used to clarify the nature of the observed spectral peaks. The frequency of a resonant oscillation depends primarily on the speed of sound and only weakly on the convective speed. A variation in Mach number with the same stagnation conditions will not substantially alter the temperature of the chamber, and thus the frequency of an acoustic free mode, if the Mach number is kept reasonably low. The variation in the flow velocity, however, is almost proportional to that in the Mach number. The frequency of a coupled-mode oscillation will then be shifted substantially with variations in the Mach number. In order to take advantage of this property, two simulations were performed: one at an inlet Mach number of 0.32, the other at 0.44. By comparing the frequency spectra of the oscillations from these two simulations, the resonant modes and the coupled modes can be identified.

The spectra of pressure oscillations at the base of the step from these two simulations are shown in Figs. 5a and 5b. The peaks in the 650-Hz range from these two simulations are almost identical. These peaks are identified as acoustic resonant oscillations. To investigate the properties of this mode further, the obtained pressure spectra at a set of discrete points along the wall of the combustion chamber were analyzed. The amplitudes of the 650-Hz peaks were plotted against the axial distance in Fig. 6. From this figure, the sonic throat appears to serve as a nodal point for this mode of oscillation. There is also another minimum in the dump region. Since the phase information was not retained, this minimum is assumed to be a node. The frequency estimate using the distance between these two node points as half of an acoustic wavelength is approximately 650 Hz, which agrees with that obtained from the spectra. The present investigation has not attempted to develop an accurate method of predicting the frequencies of the acoustic eigenmodes for the combustor combined with an inlet duct. The dump has a slenderness ratio of approximately 5 and a sonic nozzle located downstream. A one-dimensional model may not give an accurate estimate of the frequency even for the lowest few modes. The results of the numerical simulations, as shown in Fig. 6, provide an approximate mode shape for the excited acoustic resonant mode near the combustor wall. Further investigation is required to substantiate this conclusion.

Figure 5 also shows that the frequency peaks in the range of 180 and 370 Hz in the simulation with a Mach number of 0.32 (Fig. 5a) are shifted upward with the increase in Mach number to the range of 260 and 450 Hz (Fig. 5b). These are identified as the coupled-mode oscillations. Further, to substantiate that these lower-frequency peaks are related to vortex motion, the time history of vorticity was recorded at a location near the impingement point, which is identified in the vorticity contour

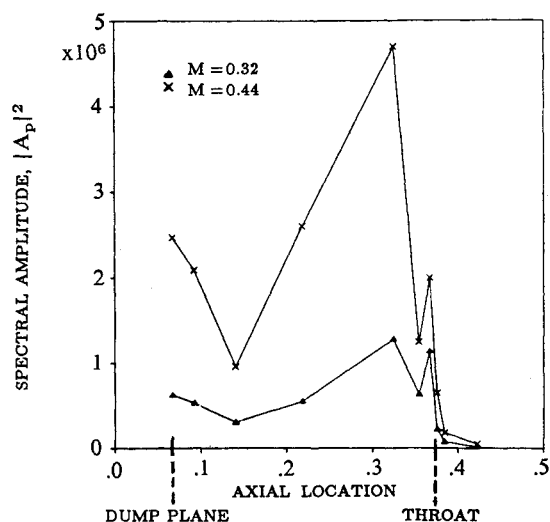


Fig. 6 Wall pressure amplitude for the 650-Hz oscillation.

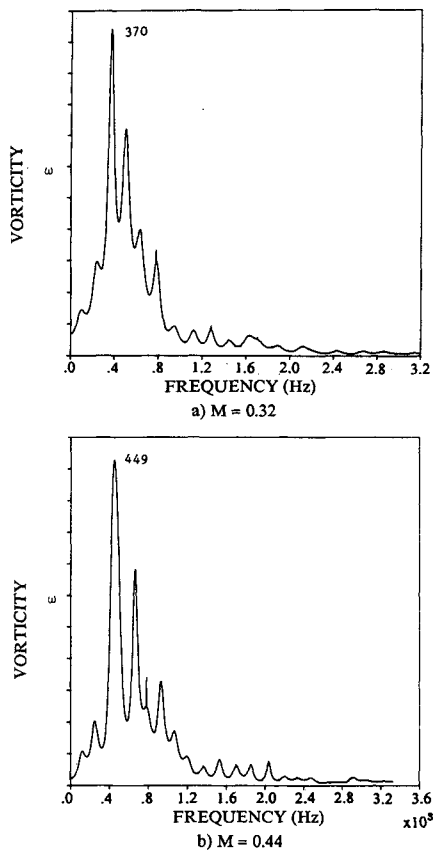


Fig. 7 Vorticity spectra near the nozzle entrance. Conditions same as in Fig. 5: a) $M = 0.32$; and b) $M = 0.44$.

plots. The power spectra of the vorticity fluctuations at these locations for the two Mach numbers are shown in Figs. 7a and 7b. In these figures, strong vortical activity is evident in the neighborhood of the low-frequency ranges of 370 and 450 Hz.

In addition, it is shown in the preceding section that, as a large vortical structure impinges on the wall, the local instantaneous fluctuating dilatation field collectively behaves as a dipole. A strong sound radiation may originate from that region. This observation suggests that the low-frequency pressure fluctuations at the base of the step appear to correlate with the vorticity impingement at the downstream nozzle. In the following section, a model to describe the coupled-mode oscillations is proposed.

Coupled-Mode Oscillation

It was demonstrated in the preceding section that, at the base of the backward-facing step, the pressure oscillation appears to contain frequency components correlating well with those of the vorticity fluctuations near the impingement point depend on the convective speed of the large vortices. This correlation suggests that the vorticity fluctuation may participate directly in the oscillation mode. Although the details of the interaction process can be quite complex, its essential mechanism may be described in the following simple manner. Upon impinging on the nozzle, a vortex generates an acoustic disturbance, which then propagates upstream and is locally amplified by the diffraction around the corner of the backward-facing step. The resulting acoustically induced velocity perturbs the shear layer near the separation point. This perturbation propagates downstream as an unstable vorticity wave, which results in the formation of a large vortical structure. The process is thus self-sustaining. This class of oscillations is referred to as the coupled mode.

Coupled-mode oscillations have been described in many different terms for various flow conditions. For example, Rockwell and Naudascher¹⁵ made an extensive review of the

self-sustaining edge-tone or cavity oscillations. Culick and Magiawala⁸ discussed the pressure oscillations in a solid-propellant rocket in which the spacer of the grain sheds vortices that, upon impinging on the downstream spacer, generate upstream-propagating acoustic disturbances that initiate new vortices. Dunlap and Brown¹⁶ and Brown et al.¹⁷ experimentally identified periodic vortex shedding as one of the primary sources of acoustic energy in a rocket engine and in a ramjet. Flandro⁶ proposed a model for the experiments by Dunlap and Brown¹⁶ and suggested that the vortex interaction with an area constriction produces an axial acoustic dipole; this conclusion is supported by the present numerical simulations.¹ Ho and Nosseir¹⁸ experimentally investigated a similar feedback mechanism for a jet impinging on a flat plate. Abouseif et al.¹⁹ studied the generations of acoustic upstream feedback by the interaction of an entropy wave with a nozzle. Martin et al.²⁰ identified a similar mechanism as the source of wind-tunnel pumping observed in an open jet tunnel with a downstream diffuser. Tam and Block²¹ investigated the origin of the pressure oscillations in a cavity with external flow. Bogar and Sajben²² used this mechanism to explain the experimentally observed oscillations in a diffuser with a frequency not associated with the acoustic modes. Williams²³ pointed out the possibility of combined vorticity/acoustic oscillations in a combustion chamber.

A model has been constructed that uses the information presented earlier in this article about the characteristics of the acoustic source resulting from the interaction between impinging vortices and the nozzle. The inlet duct is also included as a part of the acoustic system in the coupled-mode oscillations. This model not only clearly demonstrates the physical mechanism of the interaction between the acoustic wave and the vortical disturbance but also provides a method for evaluating approximately the frequencies of the coupled modes.

Equation (7) is rewritten in the following form:

$$\nabla^2 \phi = \frac{1}{c^2} \frac{D^2 \phi}{Dt^2} + \Delta' \quad (10)$$

where Δ' is the distributed dilatation field contributed by the source. As discussed the contribution of the propagation term to the dilatation field is small compared to that of the source term in the source region. Hence, the dilatation field computed from the simulations consists primarily of the latter. To investigate the propagation aspects of the acoustic wave, Eq. (10) is filtered to reveal the long-wave behavior. This results in restoration of the propagation term; the small-scale sources are compact and can be represented by the Dirac delta function or other generalized functions.

It is perhaps more illustrative to use acoustic pressure, rather than acoustic potential, as the acoustic variable for this simple one-dimensional model, i.e.,

$$\frac{1}{c^2} \frac{\partial^2 p}{\partial t^2} - \frac{\partial^2 p}{\partial x^2} = \rho \frac{\partial \Delta'}{\partial t} \quad (11)$$

In Eq. (11), the convection of acoustic disturbances by the mean flow is neglected for low subsonic flows, and Δ' is the filtered dilatation field. In the preceding discussion, it was found that a strong dipole source for dilatation is generated by the impingement of vortices on the nozzle wall. The dimensions of the nozzle are assumed to be small relative to the acoustic wavelength. Therefore, the multipole expansion of the computed dilatation field can be applied by using the entire nozzle region, from the entrance to the throat, as the sampling volume. The results can be interpreted as the acoustic response of the complete vortex/nozzle/acoustic interaction, because the dilatation field is computed by solving the nonlinear flow equations and by satisfying the exact boundary conditions on the nozzle wall. Hence, the dilatation field at the nozzle can be written as

$$\Delta' = -\alpha \Omega(x_n) (\partial/\partial x) \delta(x - x_n) \quad (12)$$

where α is a transfer coefficient, $\delta(x)$ is the Dirac delta function, and x_n is the axial location of the nozzle. The sign in Eq. (12) is determined by the fact that the dipole source is 180 deg out of phase with the vorticity fluctuations.

For a vortical disturbance, the following convective equation is assumed:

$$(\partial\Omega/\partial t) + u_0 (\partial\Omega/\partial x) = \sigma\Omega \quad (13)$$

where u_0 is the convective velocity for the vorticity. In this one-dimensional model, the detailed dynamics of the vorticity is lost. For example, the instability of a vortex sheet or a shear layer cannot be included in one-dimensional dynamics. Instead, an ad hoc model of a growth rate σ for the vorticity disturbance is included in Eq. (13) to reflect the spatial growth of a vortical disturbance. From Michalke,²⁴ the growth rate of the vortical disturbance is related to the thickness of the shear layer; it is larger for a thinner shear layer and smaller for a thicker shear layer. The convective velocity u_0 consists of two parts. The dominant part is the phase speed of the vorticity disturbance. This convective speed has been observed to be 0.5–0.6 of the exit velocity at the dump plane. In the numerical simulations, a two-point correlation of the vorticity fluctuations along the flow direction was obtained for estimating the propagation speed.¹ It was found that the convective speed for the vorticity in the dump is approximately 0.6 of the velocity in the inlet duct, as was found by many previous investigators, and becomes slower approaching the impingement point. The other part of the convective velocity is the convection of vorticity by acoustically induced velocity. This is assumed to be small and is neglected in the one-dimensional model. The generation of vortical disturbances in the interior of the combustor is neglected. The sources of generation of vortical disturbances are mainly nonlinear mechanisms, such as the interaction between an acoustic wave and an entropy wave or between an entropy wave and a vortical wave. An example of the latter can be found in the numerical simulation of a heat-releasing reacting mixing layer,²⁵ where the so-called baroclinic torque produces vorticity in the flowfield. Such mechanisms are considered small in the linearized model and are neglected in Eq. (13). The most important mechanism by which the acoustic wave perturbs the shear layer is its interaction with the corner of the backward-facing step, as will be discussed later.

The acoustic equation, i.e., Eq. (11), is applied separately to both the dump combustor region and the inlet duct. The solutions in these two regions are matched by the continuity conditions at the dump plane. Thus, if p_1 and p_2 are the solutions in the duct and the dump region, respectively, the following boundary conditions are applied:

$$p_1 = p_2 \quad \text{at } x = 0 \quad (14)$$

$$d_1^2 (\partial p_1 / \partial x) = d_2^2 (\partial p_2 / \partial x) \quad \text{at } x = 0 \quad (15)$$

where the dump plane is located at $x = 0$ and the diameters of the inlet duct and the dump are d_1 and d_2 , respectively.

Numerically, a constant stagnation-pressure boundary condition was applied at the inlet.¹ This condition can be formulated in terms of a homogeneous boundary condition by linearization of the steady-state isentropic relation as

$$\frac{p_1}{p} + \gamma M \frac{u'}{c} = 0 \quad (16)$$

where u' is the acoustic velocity and M is the Mach number at the inlet. In an unsteady calculation, the stagnation pressure, as defined by the steady-state form, is not applicable, strictly speaking. Without better implementation of the inflow boundary condition, however, this boundary condition can be considered as an ad hoc condition. It is important that this boundary condition does not add energy to the acoustic oscil-

lations in the interior of the computational domain. It was found that this boundary condition actually has a damping effect on the acoustic waves in the system and does not generate spurious acoustic waves that could otherwise be mistaken as self-sustained oscillations.

The nozzle and the supersonic region downstream of the throat are replaced by a dipole source in the acoustic equation. Because the behavior of the dipole source has been computed by the numerical simulation, the left-running waves resulting from the complex acoustic/vortex/nozzle interaction are included in the radiated waves by the source. Thus, no additional left-running "free wave" from the homogeneous solution of the acoustic equation is required.

The remaining boundary condition is the mechanism of perturbing the shear layer by an acoustic wave at the dump plane. At the step where the boundary layer separates from the surface to form a free shear layer, an acoustic disturbance is amplified locally by the diffraction around the sharp convex corner. In fact, a linear acoustic theory will predict an infinite acoustic velocity at the corner. Research in the past has been directed toward the issue of the so-called acoustic susceptibility at the separation point. For example, Orszag and Crow²⁶ addressed the problem in the incompressible limit by examining the shear layer behind a trailing edge. They found that a new vorticity disturbance must be initiated to compensate for the infinite flow velocity at the trailing edge induced by the instability wave of the vortex sheet. Crighton and Leppinton²⁷ investigated the acoustic susceptibility of the shear layer behind a trailing edge of a flat plate. Again, the Kutta condition at the trailing edge determines the vorticity disturbance that eventually grows into a large-scale coherent structure. This mechanism can be represented by the following boundary condition:

$$\Omega|_{x=0} - \beta u' = 0 \quad (17)$$

Here, β is another transfer function and u' is the acoustic induced velocity at the dump plane, which is related to the gradient of acoustic pressure by the relation

$$\rho_0 (\partial u' / \partial t) = -(\partial p_2 / \partial x) \quad (18)$$

The vorticity dynamics and the acoustic oscillations are coupled through the dipole source and the boundary condition at the dump plane. The system of equations with the boundary conditions is homogeneous. We seek an eigensolution of the form

$$\begin{bmatrix} p \\ \Omega \end{bmatrix} = \begin{bmatrix} \hat{p}(x) \\ \hat{\Omega}(x) \end{bmatrix} e^{ift} \quad (19)$$

where f is the frequency. The variables in the remainder of this article are all nondimensionalized by the reference quantities (e.g., the velocity by the speed of sound c , the spatial coordinate by x_n , time by x_n/c) and use the same nomenclature as the dimensional quantities.

The vorticity equation, i.e., Eq. (13), can be integrated easily to give

$$\hat{\Omega} = a_5 e^{(-ifx/M_0) + (\sigma/M_0)x} \quad (20)$$

where a_5 is an arbitrary integration constant, M_0 is the Mach number of the vortex convective speed, and σ represents the nondimensional growth rate of vortical disturbances.

The Green's function for the acoustic equation, i.e., Eq. (11), is given by a retarded potential as

$$G(x, x_0, t, \tau) = \delta(\tau - t + |x - x_0|) \quad (21)$$

Thus, the particular solution of Eq. (11) can be given by

$$p_p = -\alpha \frac{\partial^2}{\partial t \partial x} \int_{-\infty}^{\infty} \int_{-\infty}^{\infty} \Omega(\tau, x_n) \delta(x_0 - x_n) \times \delta(\tau - t + |x - x_n|) d\tau dx_0 \quad (22)$$

or

$$p_p = \pm \alpha \Omega'(t - |x - x_n|) \quad \begin{matrix} x < x_n \\ x > x_n \end{matrix} \quad (23)$$

where the prime denotes the derivative with respect to the argument. Only the region $x < x_n$ is of interest.

Using Eq. (23), the general solution of the forced acoustic equation in the dump region can be given as

$$\hat{p}_2 = a_3 e^{ifx} + a_4 e^{-ifx} \pm a_5 (\Lambda/\beta) F e^{-if|x-x_n|} \quad \begin{matrix} x < x_n \\ x > x_n \end{matrix} \quad (24)$$

where

$$\Lambda = \alpha \beta e^{(\sigma/M_0)x_n} \quad (25)$$

and

$$F = f^2 e^{(ifx_n/M_0)} \quad (26)$$

Here, a_3 and a_4 are integration constants. It is useful to express the derivative of p_2 as

$$\hat{p}_{2,x} = if[a_3 e^{ifx} - a_4 e^{-ifx} + a_5 (\Lambda/\beta) F e^{-if|x-x_n|}] \quad (27)$$

There is no phase shift across the nozzle.

The acoustic pressure in the inlet duct is simply given by

$$\hat{p}_1 = a_1 e^{ifx} + a_2 e^{-ifx} \quad (28)$$

where a_1 and a_2 are integration constants.

The coefficient a_3 can be set to zero to eliminate the left-running "free wave," as was discussed. The remaining integration constants can be determined by the boundary conditions given in Eqs. (14–18). Because these boundary conditions are homogeneous, the eigenvalue f can be obtained from the condition that the characteristic determinant vanishes.

The eigenvalue problem contains four physical parameters: the convective Mach number M_0 , the inlet duct length l , the area ratio between the dump and the inlet duct $R (= d_1^2/d_2^2)$, and an overall interaction parameter Λ as defined by Eq. (25). This parameter is nondimensional and reflects the overall degree of interaction between acoustic oscillations and vorticity dynamics in the system. For example, an unstable shear layer with a large growth rate σ will interact more strongly with acoustic waves. Strictly speaking, Λ is not independent of the frequency f . However, the present assumption of a constant interaction parameter probably does not affect the real part of the eigenvalue f .

The characteristic condition can be simplified to the following equation:

$$\left(\frac{R+1}{R-1} - \frac{1+M}{1-M} e^{2ifl} \right) (2\Gamma + 1) - \left(\frac{2R}{R-1} \right) (1+\Gamma) \left(1 + \frac{1+M}{1-M} e^{2ifl} \right) = 0 \quad (29)$$

where

$$\Gamma = F \Lambda e^{-if} \quad (30)$$

The frequency f is a complex number, and absolute instability is possible when $\text{Im}(f) < 0$. It can be shown that there is a stability criterion for the parameter Λ below which the system

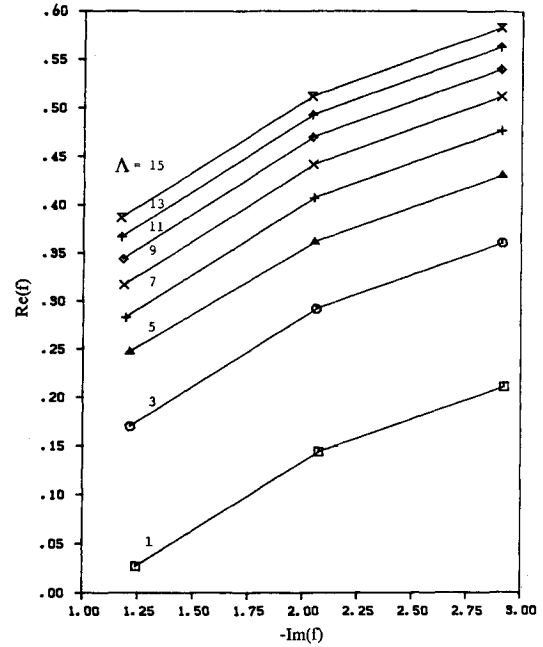


Fig. 8 Eigenvalues for the coupled mode.

is stable. For large Λ , it can be easily shown that the growth rate of the instability behaves as $\ln \Lambda$. Figure 8 shows the complex eigenfrequencies for the first three modes for various values of Λ .

The frequencies of the first two modes computed from this model problem are 190 and 360 Hz, which seem to reflect what has been observed in the numerical simulations, although there are discrepancies in the numerical values. There are quite a number of uncertainties in the model that are still considered as ad hoc assumptions. The convective speed of vortices in the dump is taken as 0.5 of the jet velocity at the dump plane. This reduced value was used in place of the value of 0.6 observed in a freejet to account for the deceleration of the vortices as they approach the impingement point, as was discussed previously.¹ Also, the convection of acoustic waves by the mean flow has been neglected. These factors can certainly affect the eigenfrequencies computed using the model. Nevertheless, this simple one-dimensional model, using the behavior of the acoustic sources extracted from the numerical simulations, is very helpful in understanding the complex physical processes involved in acoustic wave/vortex interactions.

Discussion

The pressure oscillations in a ramjet combustor under cold-flow conditions were investigated. The main contribution of this investigation is the evidence that both resonant oscillations and coupled-mode oscillations exist in the combustor. The former represent an acoustic free mode excited by vortex activities, and the latter are oscillations in which the vortical disturbances play a primary role in the formation of eigenfunctions. The amplitude of these oscillations, however, is small. To understand the origin of the large-amplitude pressure oscillations observed in an instability mode in a ramjet combustor, the chemical heat release must be included. The interaction among vortical disturbances, acoustic disturbances, entropy disturbances, and solid surfaces will be even more complex than in the present case. Both acoustic resonant modes and convective-wave/acoustic-wave coupled modes are potential candidates for combustion instability when heat release is included. The application of the methodology presented in this article and in the related study¹ to cases with heat release is now being attempted.²⁸

It is worthwhile to make a few comments on the present numerical simulations. A simulation of the phenomenon of

resonant oscillations requires a long computing time for the flowfield to evolve into a quasistationary state. Even for the present axisymmetric simulation, significant computational time is required to obtain enough data for a meaningful statistical analysis.¹ The results presented here are perhaps the limit of what can be done with state-of-the-art computing capabilities. The breakdown of the axisymmetric vortical structures into three-dimensional turbulence and the transfer of spectral energy to high wave numbers be three-dimensional vortex stretching is missing in this study. The dissipation of large vortical structures can only be partially accounted for in the present investigation by the relatively large molecular viscosity and perhaps by the numerical dissipation near the end of the combustor where the grid spacing is relatively large. The extension of the simulations to three-dimensional space requires a computer at least an order of magnitude faster. Even then, a subgrid-scale turbulence model will be required. Subgrid models for compressible flows have just been emerging,^{29,30} and need to be validated for practical applications.

Acknowledgments

The present work is supported by the Office of Naval Research under Contract No. N00014-84-C0359. This research would not have been possible without support from NASA Lewis Research Center for generous computing time on the CRAY-XMP computer, and from the National Aerodynamics Simulator (NAS) at NASA Ames Research Center for high-resolution computations. During the course of the research, comments by F. E. C. Culick of the California Institute of Technology, C.-M. Ho of the University of Southern California, and Klaus Schadow of the Naval Weapons Center have been very helpful. The first author would like to thank Morton Cooper, formerly with Flow Research, Inc., who first suggested the problem and whose encouragement on this project as well as others throughout years of collaboration has been an important source of inspiration to him.

References

- ¹Menon, S., and Jou, W.-H., "Numerical Simulations of Oscillatory Cold Flows in an Axisymmetric Ramjet Combustor," *Journal of Propulsion and Power*, Vol. 6, No. 5, 1990.
- ²Moin, P., and Kim, J., "Numerical Investigation of Turbulent Channel Flow," *Journal of Fluid Mechanics*, Vol. 118, 1982, pp. 341-377.
- ³Riley, J. J., and Metcalfe, R. W., "Direct Numerical Simulation of a Perturbed Turbulent Mixing Layer," AIAA Paper 80-0274, 1980.
- ⁴Chu, B.-T., and Kovaszny, L. S. G., "Nonlinear Interactions in a Viscous Heat-Conducting Compressible Gas," *Journal of Fluid Mechanics*, Vol. 3, 1958, pp. 494-514.
- ⁵Goldstein, M. E., *Aeroacoustics*, McGraw-Hill, New York, 1976.
- ⁶Flandro, G. A., "Vortex Driving Mechanism in Oscillatory Rocket Flows," *Journal of Propulsion and Power*, Vol. 2, No. 3, 1986, pp. 206-214.
- ⁷Crighton, D. G., "The Excess Noise Field of Subsonic Jets," *Journal of Fluid Mechanics*, Vol. 56, 1972, pp. 683-694.
- ⁸Culick, F. E. C., and Magiawala, K., "Excitation of Acoustic Modes in a Chamber by Vortex Shedding," *Journal of Sound and Vibration*, Vol. 64, 1979, pp. 455-457.
- ⁹Lighthill, M. J., "On Sound Generated Aerodynamically—I. General Theory," *Proceedings of the Royal Society (London), Series A*, Vol. 211, 1952, pp. 564-587.
- ¹⁰Yates, J. E., "Application of the Bernoulli Enthalpy Concept to the Study of Vortex Noise and Jet Impingement Noise," NASA CR 2987, 1977.
- ¹¹Crow, S. C., "Aerodynamic Sound Emission as a Singular Perturbation Problem," *Studies in Applied Mathematics*, Vol. 49, 1970, pp. 21-44.
- ¹²Ffowes Williams, J. E., "Hydrodynamic Noise," *Annual Review of Fluid Mechanics*, Vol. 1, 1969, pp. 197-222.
- ¹³Wills, J. A. B., "Measurements of the Wave-Number/Phase-Velocity Spectrum of Wall Pressure Beneath a Turbulent Boundary Layer," *Journal of Fluid Mechanics*, Vol. 45, 1970, pp. 65-90.
- ¹⁴Ffowes Williams, J. E., "Boundary-Layer Pressures and the Corcos Model: A Development to Incorporate Low-Wavenumber Constraints," *Journal of Fluid Mechanics*, Vol. 125, 1982, pp. 9-25.
- ¹⁵Rockwell, D., and Naudascher, E., "Self-Sustained Oscillations of Impinging Free Shear Layers," *Annual Review of Fluid Mechanics*, Vol. 11, 1979, pp. 67-94.
- ¹⁶Dunlap, R., and Brown, R. S., "Exploratory Experiments on Acoustic Oscillations Driven by Periodic Vortex Shedding," *AIAA Journal*, Vol. 19, No. 3, 1981, pp. 408-409.
- ¹⁷Brown, R. S., Dunlap, R., and Young, S. W., "Vortex Shedding Studies in a Simulated Coaxial Dump Combustor," *Journal of Propulsion*, Vol. 1, No. 5, 1985, pp. 413-415.
- ¹⁸Ho, C.-M., and Nosseir, N. S., "Dynamics of Impinging Jets; Pt. I—The Feedback Mechanism," *Journal of Fluid Mechanics*, Vol. 105, 1981, pp. 119-142.
- ¹⁹Abouseif, G. E., Keklak, J. A., and Toong, T. Y., "Ramjet Rumble: The Low-Frequency Instability Mechanism in Coaxial Dump Combustors," *Combustion Science and Technology*, Vol. 36, 1984, pp. 83-108.
- ²⁰Martin, R. M., Brooks, T. F., and Hoad, D. R., "Reduction of Background Noise Induced by Wind-Tunnel Jet Exit Vanes," *AIAA Journal*, Vol. 23, 1985, pp. 1631-1632.
- ²¹Tam, C. K., and Block, P. J. W., "On the Tones and Pressure Oscillations Induced by Flow over Rectangular Cavities," *Journal of Fluid Mechanics*, Vol. 89, Pt. 2, 1978, pp. 373-399.
- ²²Bogar, T. J., and Sajben, M., "The Role of Convective Perturbations in Supercritical Inlet Oscillation," CPIA Publication No. 412, Vol. 1, 1979, p. 465.
- ²³Williams, F. A., *Combustion Theory*, 2nd ed., Benjamin/Cummings Publishing, Menlo Park, CA, 1985.
- ²⁴Michalke, A., "The Instability of Free Shear Layers: A Survey on the State of the Art," *Progress in Aerospace Sciences*, Vol. 12, 1972, pp. 213-239.
- ²⁵McMurtry, P., Jou, W.-H., Riley, J., and Metcalfe, R., "Direct Numerical Simulations of a Reacting Mixing Layer with Chemical Heat Release," *AIAA Journal*, Vol. 24, 1986, pp. 962-970.
- ²⁶Orszag, S. A., and Crow, S. C., "Instability of a Vortex Sheet Leaving a Semiinfinite Plate," *Studies in Applied Mathematics*, Vol. 49, 1970, pp. 167-181.
- ²⁷Crighton, D. G., and Leppinton, F. G., "Radiation Properties of the Semi-Infinite Vortex Sheet: The Initial-Value Problem," *Journal of Fluid Mechanics*, Vol. 64, 1974, pp. 393-414.
- ²⁸Menon, S., and Jou, W.-H., "Large-Eddy Simulations of Combustion Instability in an Axisymmetric Ramjet Combustor," AIAA Paper 90-0267, Jan. 1990; (to be published in *Combustion Science and Technology*).
- ²⁹Erlebacher, G., Hussaini, M. Y., Speziale, C. G., and Zang, T. A., "Towards the Large-Eddy Simulation of Compressible Turbulent Flows," Institute for Computer Applications in Science and Engineering, Hampton, VA, ICASE Rept. 87-20, 1987.
- ³⁰Yoshizawa, A., "Statistical Theory for Compressible Turbulent Shear Flows, with Application to Subgrid Modeling," *Physics of Fluids*, Vol. 29, 1986, pp. 2152-2164.